JOURNAL OF Materials CHEMISTRY

Influence of reaction conditions on the electrochemical–hydrothermal synthesis of two ammonium vanadium phosphates: $(NH_4)_2VO(HPO_4)_2{\cdot}H_2O$ and $(NH_4)_2VO(V_{0.88}P_{1.12}O_7)$

Lumei Liu, Xiqu Wang, Ranko Bontchev, Kent Ross and Allan J. Jacobson

Department of Chemistry, University of Houston, Houston, TX 77204–5641, USA. E-mail: ajjacob@uh.edu

Received 11th March 1999, Accepted 19th April 1999

The new phase $(NH_4)_2VO(HPO_4)_2{\cdot}H_2O$, **1**, has been synthesized by hydrothermal electrocrystallization at 100 °C. **1** is triclinic, space group $P\bar{1}$ with $Z=2$, $a=7.2499(8)$, $b=8.1244(9)$, $c=8.6529(9)$ Å, $\alpha=73.472(2)$, $\beta=80.085(2)$, $\gamma=85.077(2)^\circ$ and $V=480.94(9)$ Å^3. When the reaction temperature is increased to 110 °C, **1** is completely transformed into the known compound $(NH_4)_2VO(V_{0.88}P_{1.12}O_7)$, **2**. The layered compound $NH_4VOPO_4{\cdot}xH_2O$, **3**, a new example of the well-known $M_xVOPO_4{\cdot}xH_2O$ phase has also been prepared by the same technique.

Introduction

Recently, electrocrystallization under hydrothermal conditions has been used successfully for the synthesis of thin films[1] of, for example, $BaTiO_3$,[2] $BaMoO_4$[3] and $LiNiO_2$.[4] We are investigating the adaptation of this approach to the exploratory synthesis of new phases and for the growth of single crystals. We have previously reported the syntheses and single crystal structural characterization of the new phases $BaV_7O_{16}{\cdot}nH_2O$,[5] $Zn_2(OH)VO_4$[6] and $[N(CH_3)_4]_2[Co(H_2O)_4V_{12}O_{28}]$[7] by electrochemical oxidation of vanadium metal anodes at 170 °C. We have extended these studies to investigate electrochemical oxidation of vanadium at lower temperatures (100–110 °C) and report herein syntheses in the presence of $(NH_4)_2HPO_4$ as a function of solution pH.

A number of ammonium vanadium phosphate phases have been reported in the literature including, α– and β–$NH_4V^VO_2HPO_4$,[8,9] $(NH_4)_2V^{IV}O(V^V_{2-x}P_xO_7)$,[10] $NH_4V^{IV}OPO_4$,[11] $NH_4V^{IV}OPO_4{\cdot}H_2O$,[12] $(NH_4)_2V^{IV}OP_2O_7$,[13] α–$(NH_4)_2(V^{IV}O)_3(P_2O_7)_2$,[13] α– and β–$NH_4V^{III}(HPO_4)_2$[14,15] and $NH_4V^{III}P_2O_7$.[13] We have synthesized the new phase $(NH_4)_2VO(HPO_4)_2{\cdot}H_2O$, **1**, by hydrothermal electrocrystallisation at 100 °C. When the reaction temperature is increased to 110 °C, **1** is completely transformed into the known compound $(NH_4)_2VO(V_{0.88}P_{1.12}O_7)$, **2**.[10] The layered compound $NH_4VOPO_4{\cdot}xH_2O$, **3**, a new example of the well-known $M_xVOPO_4{\cdot}xH_2O$ phase,[16,17] has also been prepared.

Experimental

Synthesis

The syntheses of compounds **1**, **2** and **3** were performed using screw top plastic containers (volume, 80 mL) fitted with feedthroughs for electrical connections between the external circuit and the electrodes inside the reaction chamber. The transparent container wall allows visual inspection of the electrodes during the reaction. In a typical synthesis of **1**, 40 mL of a 0.5 M solution of $(NH_4)_2HPO_4$ was sealed in the container in air. The initial pH was adjusted to 8.0 with ammonium hydroxide and fell slowly during the course of the reaction to *ca.* 7.2. The anode (working electrode) was a vanadium metal plate ($20\times10\times0.254$ mm). A gold foil was used as cathode (counter electrode). The experiment was conducted with current densities of *ca.* 1–3 mA generated by using a commercial power source (MacPile, Biologic Scientific Instruments) at 100 °C for 167 h. A sheet of green crystals of compound **1** was formed on the vanadium electrode. In a similar reaction, but at 107 °C, electrolysis (232 h) of a 0.5 M $(NH_4)_2HPO_4$ solution with an initial pH of 7.9 (final pH = 6.7) gave only red crystals of **2** on the vanadium electrode. The effect of temperature on product formation was confirmed by starting an experiment at 100 °C and then subsequently raising the temperature to 110 °C. The green crystals of **1** formed at 100 °C were completely converted at 110 °C to red crystals of **2** on the anode surface.

Additional reactions were carried out under similar conditions to those described above, but at lower pH. At pH = 5 and 110 °C in 0.5 M $(NH_4)_2HPO_4$, electrocrystallization for 212 h led to the formation of **3** as a green polycrystalline solid which did not adhere to the electrode. Reaction at pH 2 also led to the formation of microcrystalline solids. Two distinct phases were identified from powder X-ray diffraction patterns but were not characterized further.

X-Ray crystallography

For single crystal X-ray data collection, a platy crystal of **1** with approximate dimensions $0.09\times0.04\times0.02$ mm was mounted on a glass fiber using silicone sealant. Intensities were measured on a SMART platform diffractometer equipped with a 1 K CCD area detector using graphite-monochromatized Mo-Kα radiation at room temperature. A hemisphere of data (1271 frames at 5 cm detector distance) was collected using a narrow-frame method with scan widths of 0.30° in ω and an exposure time of 30 s frame^{-1}. The first 50 frames were re-measured at the end of data collection to monitor instrument and crystal stability, and the maximum correction applied on the intensities was $<1\%$. The data were integrated using the Siemens SAINT program,[18] with the intensities corrected for Lorentz factor, polarization, air absorption and absorption due to variation in the path length through the detector faceplate. Final cell constants were refined using 1504 reflections having $I>10\sigma(I)$. An empirical absorption correction was made using the SADABS program.[19]

The structure was solved by direct methods and refined using SHELXTL.[20] All non-hydrogen atom positions were derived by direct methods. The V and P atoms were refined anisotropically. Anisotropic refinement of the oxygen and nitrogen atoms was not successful, probably because of the poor crystal quality (small size). Many other crystals of larger dimensions were examined but none proved suitable for data collection. The oxygen and nitrogen atoms were refined isotropically. No effort was made to locate the hydrogen pos-

Table 1 Crystal and structure refinement data for $(NH_4)_2VO(HPO_4)_2{\cdot}H_2O$

Empirical formula	$H_{12}N_2O_{10}P_2V$
Formula weight	313.00
Temperature/K	293(2)
Space group	*P*1
Unit cell dimensions	
a/Å	7.2499(8)
b/Å	8.1244(9)
c/Å	8.6529(9)
α/°	73.472(2)
β/°	80.085(2)
γ/°	85.077(2)
Volume/Å^3, *Z*	480.94(9), 2
Wavelength/Å	0.71073
Absorption coefficient/mm^{-1}	1.410
Reflections collected	3034
Independent reflections	2509 [R(int) = 0.0594]
Final *R* indices [$I > 2(I)$][a]	$R1 = 0.0797$, $wR2 = 0.1937$
R indices (all data)	$R1 = 0.1001$, $wR2 = 0.2045$

[a] $R1 = \sum||F_o| - |F_c||/\sum|F_o|$, $wR2 = [\sum w(F_o^2 - F_c^2)^2/(\sum wF_o^2)^2]^{1/2}$, $w = 1/(\sigma F_o^2)^2$, $w = 1/[\sigma^2(F_o^2) + (0.098P)^2]$, where $P = (F_o^2 + 2F_c^2)/3$.

itions. Discrimination between water oxygen and nitrogen atoms was made, although not unambiguously, according to their relations to other atoms. Crystallographic and refinement details are summarized in Table 1. Atom positions are given in Table 2 and selected bond lengths in Table 3.

Full crystallographic details, excluding structure factors, have been deposited at the Cambridge Crystallographic Data Centre (CCDC). See Information for Authors, 1999, Issue 1. Any request to the CCDC for this material should quote the full literature citation and the reference number 1145/155.

See http://www.rsc.org/suppdata/jm/1999/1585/ for crystallographic files in .cif format.

A red cube-shaped crystal of **2** with dimensions of $0.08 \times 0.08 \times 0.07$ mm was also mounted on the diffractometer.

Table 2 Atomic coordinates ($\times 10^4$) and equivalent isotropic displacement parameters (Å$^2 \times 10^3$) for $(NH_4)_2VO(HPO_4)_2{\cdot}H_2O$. U_{eq} is defined as one third of the trace of the orthogonalized U_{ij} tensor

Atom	*x*	*y*	*z*	U_{eq}
V(1)	3175(3)	5823(3)	8613(3)	14(1)
V(2)	8236(3)	5514(3)	8602(3)	11(1)
P(1)	10698(5)	8410(4)	5962(4)	10(1)
P(2)	6016(5)	4669(4)	5875(4)	9(1)
P(3)	5096(5)	2931(4)	11262(4)	9(1)
P(4)	−137(5)	7359(5)	10938(4)	11(1)
O(1)	7057(13)	3590(12)	10348(12)	15(2)
O(2)	5239(12)	6570(11)	8626(11)	8(2)
O(3)	4460(13)	3906(13)	12626(12)	17(2)
O(4)	4027(12)	4710(12)	6821(11)	12(2)
O(5)	11450(15)	7629(13)	4512(13)	21(2)
O(6)	439(13)	4739(11)	8548(11)	10(2)
O(7)	8769(13)	7669(11)	6777(11)	11(2)
O(8)	3580(13)	3480(12)	10154(12)	13(2)
O(9)	2187(12)	7919(11)	7096(11)	10(2)
O(10)	7552(13)	4426(12)	7004(11)	12(2)
O(11)	1725(12)	6461(11)	10493(11)	9(2)
O(12)	5192(14)	1051(12)	12039(12)	16(2)
O(13)	8237(12)	6804(11)	10232(11)	9(2)
O(14)	89(14)	9307(13)	10309(13)	22(2)
O(15)	10456(14)	10354(13)	5320(13)	19(2)
O(16)	−642(14)	6792(13)	12826(13)	22(2)
O(17)	6272(12)	3253(12)	5027(11)	11(2)
O(18)	6296(12)	6508(12)	4572(11)	12(2)
N(1)	5441(16)	9825(15)	5350(14)	15(3)
N(2)	121(17)	1748(16)	1947(15)	17(3)
N(3)	11259(17)	13656(15)	5283(15)	18(3)
N(4)	4614(16)	7861(14)	11683(14)	12(3)
OW1	7622(18)	751(17)	8192(16)	42(4)
OW2	3471(16)	744(15)	8475(15)	29(3)

Table 3 Selected bond lengths (Å) for $(NH_4)_2VO(HPO_4)_2{\cdot}H_2O$

V(1)–O(2)	1.665(9)	P(1)–O(7)	1.542(10)
V(1)–O(11)	1.955(9)	P(1)–O(5)	1.559(11)
V(1)–O(4)	1.994(10)	P(2)–O(17)	1.515(10)
V(1)–O(9)	1.995(9)	P(2)–O(4)	1.533(9)
V(1)–O(8)	2.020(10)	P(2)–O(10)	1.569(10)
V(1)–O(6)	2.254(10)	P(2)–O(18)	1.599(9)
V(2)–O(6)	1.664(9)	P(3)–O(12)	1.484(10)
V(2)–O(1)	1.974(10)	P(3)–O(8)	1.537(10)
V(2)–O(13)	1.982(10)	P(3)–O(1)	1.561(10)
V(2)–O(10)	1.987(10)	P(3)–O(3)	1.585(11)
V(2)–O(7)	2.011(9)	P(4)–O(11)	1.521(9)
V(2)–O(2)	2.266(9)	P(4)–O(14)	1.533(11)
P(1)–O(15)	1.524(11)	P(4)–O(16)	1.552(11)
P(1)–O(9)	1.535(9)	P(4)–O(13)	1.570(10)

Refinement of the structure confirmed that **2** is identical to the known phase $(NH_4)_2VO(V_xP_{2-x}O_7)$.[10] The data were refined in space group *P*4*bm* with $R(F) = 0.065$ for 363 observed reflections and 40 parameters. The details of the structure are similar to those previously reported and are not given here.[10]

The general features of the structure of **3** were deduced from the X-ray powder diffraction data. The data were indexed with a body-centered tetragonal unit cell with lattice parameters $a = 6.31$ and $c = 13.57$ Å. An analysis of the powder X-ray diffraction intensities confirmed that **3** is a member of the $M_xVOPO_4{\cdot}nH_2O$ family of layered compounds. The structure of **3** has recently been confirmed by refinement of single crystal X-ray data from a sample prepared by conventional hydrothermal synthesis.[21]

Characterization

Electron microprobe analyses were carried out with a JEOL JXA-8600 Electron Microprobe at 15 keV, 10 μm beam diameter and 30 nA beam current. Infrared spectra (KBr pellet method) were recorded on a Galaxy FTIR 5000 series spectrometer. Thermogravimetric analyses of **1**, **2** and **3** were carried out in air at a heating rate of 2 °C min^{-1} by using a TA Instruments TGA 2950 Thermogravimetric Analyzer. Powder X-ray diffraction patterns were obtained using a Scintag XDS2000 diffractometer and Cu-Kα radiation.

Results and discussion

Synthesis and characterization

Fig. 1 shows vanadium electrodes on removal from the solution after the electrocrystallization reactions. Fig. 1(a) is an optical micrograph showing a densely packed layer of crystals of **1**. Fig. 1(b) and (c) are scanning electron micrographs of **1** and **2**, respectively, showing well developed faceted crystals growing directly in contact with the vanadium sheet electrode.

Electron microprobe analysis of **1** gave a V:P ratio of $1:2.00 \pm 0.02$ and qualitatively indicated the presence of nitrogen. Thermogravimetric analysis data for **1** in air (Fig. 2) showed a sharp weight loss which began at *ca.* 100 °C, was complete by 171 °C and had a maximum rate at 151 °C. Further weight losses occurred in two overlapping steps between 170 and 600 °C. The total weight loss (27.7%) is consistent with the composition $(NH_4)_2VO(HPO_4)_2{\cdot}H_2O$ (28.2% calculated for a final product VP_2O_7). The weight loss in the first step (5.6%) corresponds to the loss of one molecule of water per formula unit (calc. 5.8%).

Thermogravimetric analysis of **2** (Fig. 2) showed a single weight loss which began at 250 °C and was complete by 375 °C. The observed weight loss of 16.7% is in reasonable agreement with the value calculated for decomposition to a mixture of P_2O_5, VO_2 and V_2O_5, with the same average vanadium oxidation state in the product as in the starting material (17.7%).

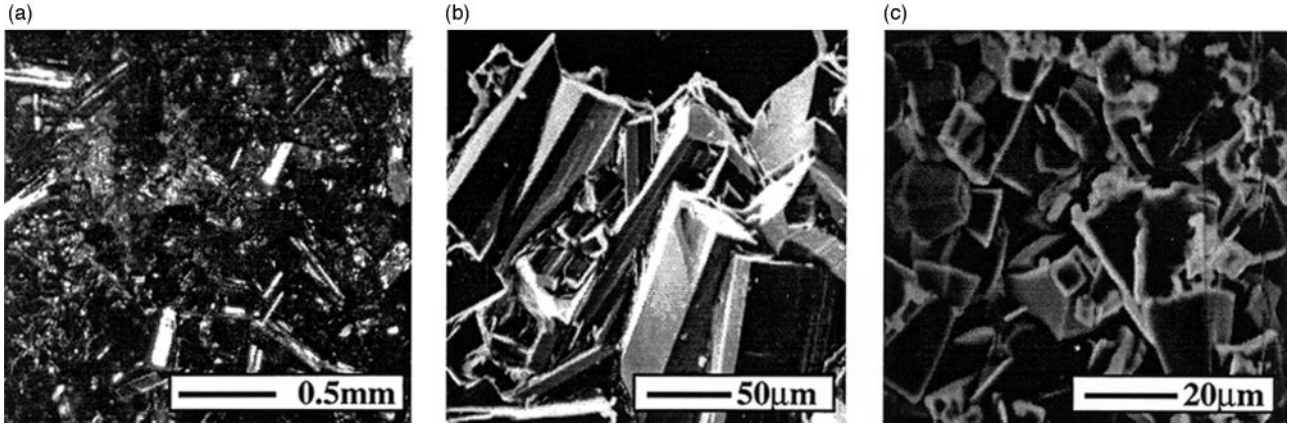

Fig. 1 Micrographs of vanadium electrodes showing densely packed layers of crystals: (a) an optical micrograph of **1**; (b) a scanning electron micrograph of **1**; (c) a scanning electron micrograph of **2**.

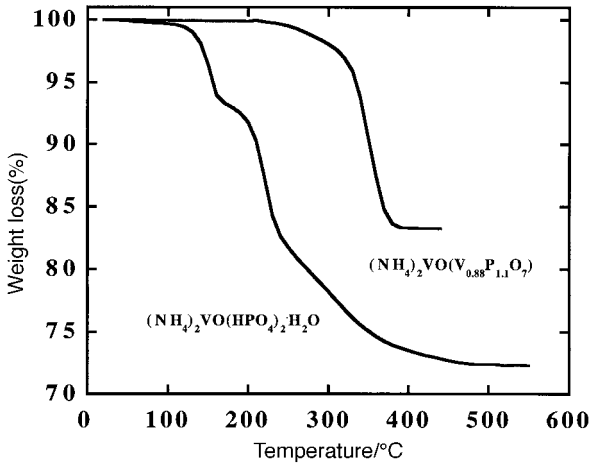

Fig. 2 Thermogravimetric analysis data for $(NH_4)_2VO(HPO_4)_2{\cdot}H_2O$ and $(NH_4)_2VO(V_{0.88}P_{1.12}O_7)$.

The difference is probably due to partial oxidation of V(IV) to V(V) during the decomposition reaction, which was carried out in air.

Thermogravimetric analysis of **3** showed a series of weight losses up to 400 °C corresponding to loss of NH_3 and H_2O. A small weight gain was observed above 420 °C. The final product was shown by X-ray powder diffraction to be β-$VOPO_4$. Analysis of the overall weight loss indicated a composition of $NH_4VOPO_4{\cdot}1.4H_2O$ assuming that **3** contains only V(IV).

The infrared spectra of **1**, **2** and **3** are shown in Fig. 3. Bands characteristic of ammonium ions (*ca.* 1400 cm^{-1}) and phosphate ions (900–1100 cm^{-1}, stretching, and 400–700 cm^{-1}, bending) and water molecules are observed (*ca.* 1650 cm^{-1} and 3550–3200 cm^{-1}, **1** and **3**). The expected V=O stretching vibrations at 990 cm^{-1} are not resolved from the phosphate bands. The infrared spectrum of **3** is identical to that of $NH_4VOPO_4{\cdot}1.5H_2O$ recently prepared by hydrothermal synthesis. The composition and structure of the latter were determined by refinement of single crystal X-ray data.[21]

The homogeneity of the electrochemically deposited samples of **1** and **2** was confirmed by comparing the X-ray powder diffraction patterns of ground samples with simulated patterns generated by using the refined atom positions and lattice constants obtained from the single crystal data.

Structure description

Views of the structure of $(NH_4)_2VO(HPO_4)_2{\cdot}H_2O$, **1**, are shown in Fig. 4 and 5. The structure consists of infinite $[VO(HPO_4)_2]$ chains running along the [100] direction with NH_4 cations and H_2O molecules located between the chains.

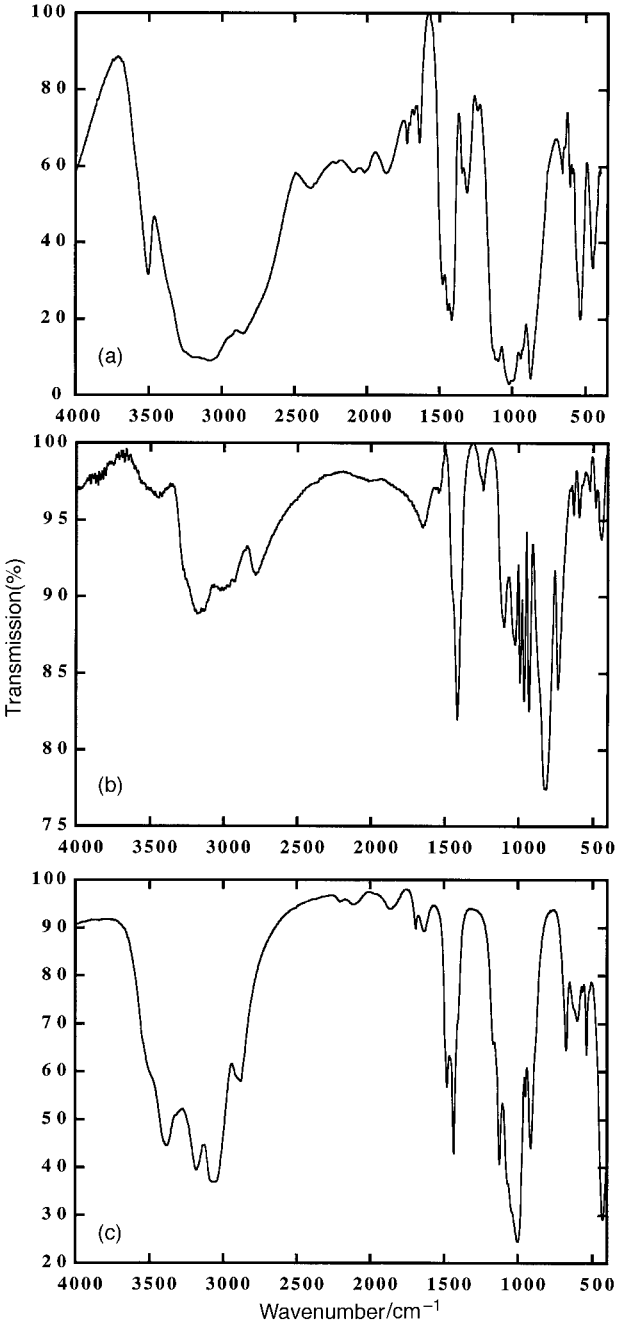

Fig. 3 IR spectra of (a) $(NH_4)_2VO(HPO_4)_2{\cdot}H_2O$ **1**; (b) $(NH_4)_2VO(V_{0.88}P_{1.12}O_7)$ **2**; (c) $NH_4VOPO_4{\cdot}xH_2O$ **3**.

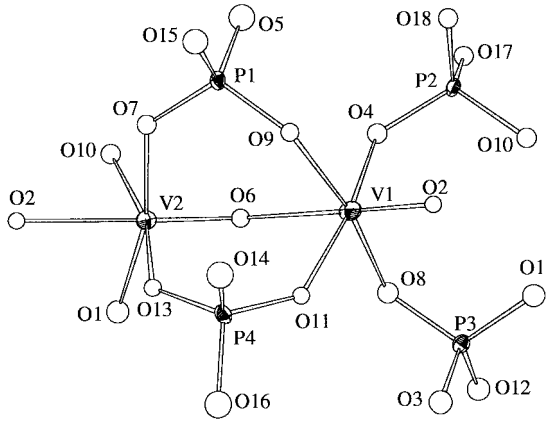

Fig. 4 A view of the local coordination environments of vanadium and phosphorus atoms in **1**. Thermal ellipsoids are plotted with 50% probability.

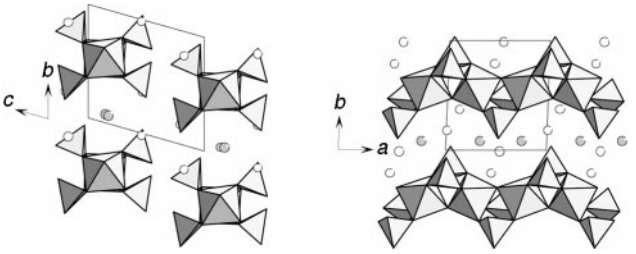

Fig. 5 Two views of the structure of $(NH_4)_2VO(HPO_4)_2{\cdot}H_2O$ **1**. The open and shaded circles are ammonium cations and water molecules, respectively.

The two non-equivalent $V(1)O_6$ and $V(2)O_6$ octahedra are very similar, each having a short V=O bond, 1.665 and 1.664 Å, respectively, *trans* to a long V–O bond, 2.254 and 2.266 Å, respectively. The octahedra share the opposed corners to form the −V=O−V=O− backbone of the infinite chain. Other V–O bond lengths are in the range 1.955–2.020 Å. Bond valence sums calculated with empirical parameters are 3.95 and 3.96 valence units for the V(1) and V(2) atoms, respectively, which are consistent with their typical V^{4+} bonding features. Adjacent VO_6 octahedra are bridged by two phosphate tetrahedra by sharing two corners of each tetrahedron.

Infinite vanadium phosphate chains similar to those of **1** have been found in the structure recently reported for $(H_3NCH_2CH_2NH_3)[V(OH)(HPO_4)_2]{\cdot}H_2O$, **4**.[22] In **4** the vanadium atoms are trivalent and form almost regular VO_6 octahedra. Therefore, the chains have a −V−OH−V−OH− backbone with uniform V–O distances. The V–O–V distances and V-O-V angles in **1** (3.61, 3.65 Å; 134.0, 136.3°) are slightly larger than those in **4** (3.61 Å, 131.3°). Both **1** and **4** crystallized in the triclinic system. However, unlike the chains in **4** which have inversion centers at the V positions, the chains in **1** are asymmetric due to the strong deformation of the VO_6 octahedra required by the V^{4+} cations. This asymmetric feature is maintained in the packing of the chains, giving rise to an asymmetric structure.

The structure of **1** is closely related to that of $(H_2NC_4H_8NH_2)[(VO)_2(HAsO_4)_2(H_2AsO_4)_2]{\cdot}H_2O$, **5**,[23] which contains infinite vanadium arsenate chains also with a −V=O−V=O− backbone. The orientation of the bridging tetrahedra in **5** is quite different from that in **1**. One-dimensional chains structurally similar to those of **1**, **4** and **5** are also found in compounds not containing vanadium. Examples include synthetic $Na_4Al(OH)(PO_4)_2$[24] and $(H_3NCH_2CH_2NH_3)$-$[Fe(OH)(HPO_4)_2]{\cdot}H_2O$,[25] and the natural minerals[26] tancoite $LiNa_2HAl(PO_4)_2(OH)$, overite $Ca_2Mg_2[Al(PO_4)_2(OH)]_2{\cdot}8H_2O$, sideronatrite $Na_2[Fe(SO_4)_2(OH)]{\cdot}3H_2O$ and metasideronatrite $Na_2[Fe(SO_4)_2(OH)]$. Recently, a vanadium phosphonate designated as MIL-10 has been reported. [27] MIL-10 contains $V^{IV}O[OP_3–CH_2–PO_3]$ chains with a −V=O−V=O− backbone. The chains are closely related to those in compound **1** (Fig. 6) but differ in that each of the two bridging tetrahedra are linked by a CH_2 group.

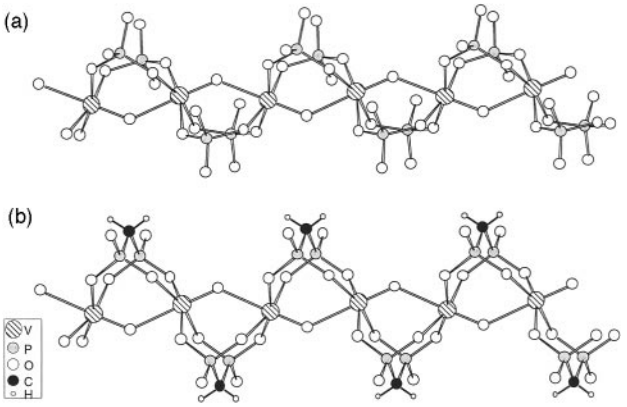

Fig. 6 Comparison of the −V−O−V− chains in (a) $(NH_4)_2$-$VO(HPO_4)_2{\cdot}H_2O$ and (b) $(NH_4)_2VO[OP_3CH_2PO_3]$.[27]

Compound **2** has a layered structure and is one member of a group of vanadates and vanado-phosphates isostructural with the mineral fresnoite, $Ba_2TiSi_2O_8$.[28] In view of the major structural difference between **1** and **2**, it is perhaps surprising that they can be inter-converted with such a small change in synthesis conditions.

Conclusions

Electrochemical oxidation of vanadium electrodes at 100–110 °C in aqueous $(NH_4)_2HPO_4$ results in the formation of several vanadium phosphate and hydrogen phosphate phases as a function of the pH of the reactions. In acidic solutions (pH = 2 or 5) microcrystalline phases are formed by precipitation from solution as the concentration of soluble vanadium species increases. By contrast, in basic solutions, crystals of **1** and **2** are formed in direct contact with the vanadium electrode most probably by the mechanism proposed by Kajiyoshi and Yoshimura[29] for $ATiO_3$ (A = Ba, Sr) film growth. In this mechanism, crystals grow by diffusion of solution species through the porous growing film to react with a thin conducting metal oxide layer formed on the metal electrode. Preliminary X-ray photoelectron spectra confirm the presence of an approximately 10 nm thick film of a reduced vanadium oxide between the metal and the layer of crystals. Growth of crystals of **1** and **2** most likely occurs *via* a similar mechanism.

Acknowledgements

This work was supported by the National Science Foundation under Grant DMR-9214804 and by the Robert A. Welch Foundation. The work made use of MRSEC/TCSUH Shared Experimental Facilities supported by the National Science Foundation under Award Number DMR-9632667 and the Texas Center for Superconductivity at the University of Houston. We thank P. van der Heide for providing the X-ray photoelectron spectra.

References

1 M. Yoshimura, W. Suchanek and K.-S. Han, *J. Mater. Chem.*, 1999, **9**, 77.
2 S. E. Yoo, M. Yoshimura and S. Somiya, *J. Mater. Sci. Lett.*, 1989, **8**, 530.
3 W.-S. Cho and M. Yoshimura, *Jpn. J. Appl. Phys.*, 1997, **36**, 1216.

4 K.-S. Han, P. Krtil and M. Yoshimura, *J. Mater. Chem.*, 1998, **8**, 2043.
5 X. Wang, L. Liu, R. Bontchev and A. J. Jacobson, *Chem. Commun.*, 1998, 1009.
6 X. Wang, L. Liu and A. J. Jacobson, *Z. Anorg. Allg. Chem.*, 1998, **624**, 1977.
7 X. Wang, L. Liu, A. J. Jacobson and K. Ross, *J. Mater. Chem.*, 1999, **9**, 859.
8 P. Amorós and A. Le Bail, *J. Solid State Chem*., 1992, **97**, 283.
9 P. Amorós, D. Beltran-Porter, A. Le Bail, G. Férey and G. Villeneuve, *Eur. J. Solid State Inorg. Chem*., 1988, **25**, 599.
10 C. Ninclaus, R. Retoux, D. Riou and G. Férey, *J. Solid State Chem*., 1996, **122**, 139; S. Boudin, A. Grandin, P. Labbe and B. Raveau, *Acta Crystallogr.*, *Sect. C*, 1996, **52**, 2668.
11 R. C. Haushalter, Q. Chen, V. Soghomonian, J. Zubieta and C. J. O'Connor, *J. Solid State Chem*., 1994, **108**, 128.
12 Z. Bircsk and W. T. A. Harrison, *Inorg. Chem.*, 1998, **37**, 5387.
13 J. Trommer, H. Worzala, S. Rabe and M. Schneider, *J. Solid State Chem*., 1998, **136**, 181.
14 R. C. Haushalter, Z. Wang, M. E. Thompson and J. Zubieta, *Inorg. Chim. Acta*, 1995, **232**, 83.
15 Z. Bircsk and W. T. A. Harrison, *Acta Crystallogr.*, *Sect. C*, 1998, **54**, 1195.
16 A. J. Jacobson, J. W. Johnson, J. F. Brody, J. C. Scanlon and J. T. Lewandowski, *Inorg. Chem.*, 1985, **24**, 1782.
17 M. Roca, M. D. Marcos, P. Amorós, J. Alamo, A. Beltrán-Porter and D. Beltrán-Porter, *Inorg. Chem*., 1997, **36**, 3414.
18 SAINT, Program for Data Extraction and Reduction, Siemens Analytical X-ray Instruments Inc., Madison, WI 53719, 1994–1996.
19 G. M. Sheldrick, SADABS, Program for Siemens Area Detector Absorption Corrections, University of Göttingen, Germany, 1997.
20 G. M. Sheldrick, SHELXTL, Program for Refinement of Crystal Structures, Siemens Analytical X-ray Instruments Inc., Madison, WI 53719, 1994.
21 J. Do, R. Bontchev and A. J. Jacobson, unpublished results.
22 Y. Zhang, C. J. Warren, A. Clearfield and R. C. Haushalter, *Polyhedron*, 1998, **17**, 2575.
23 R. C. Haushalter, Z. Wang, L. M. Meyer, S. S. Dhingra, M. E. Thompson and J. Zubieta, *Chem.Mater.*, 1994, **6**, 1463.
24 M. P. Attfield, R. E. Morris, I. Burshtein, C. F. Campana and A. K. Cheetham, *J. Solid State Chem*., 1995, **118**, 412.
25 Z. A. D. Lethbridge, P. Lightfoot, R. E. Morris, D. S. Wragg, P. A. Wright, A. Kvick and G. Vaughan, *J. Solid State Chem*., 1995, **142**, 455.
26 F. C. Hawthorne, *Am. Mineral*., 1985, **70**, 455.
27 C. Ninclaus, C. Serre, D. Riou and G. Férey, *C. R. Acad. Sci. Ser. II*, 1998, **1**, 551.
28 P. B. Moore and J. Louisnathan, *Science*, 1967, **156**, 1361.
29 K. Kajiyoshi and M. Yoshimura, *Eur. J. Solid State Inorg. Chem.*, 1996, **33**, 623.

Paper 9/01956A